Molecular Therapy
Methods & Clinical Development
Original Article

Intralingual and Intrapleural AAV Gene Therapy Prolongs Survival in a SOD1 ALS Mouse Model

Allison M. Keeler,[1,2,3] Marina Zieger,[1,2,3] Carson Semple,[3] Logan Pucci,[5] Alessandra Veinbachs,[3] Robert H. Brown, Jr.,[3,4] Christian Mueller,[2,3] and Mai K. ElMallah[1,2,3,5]

[1]Division of Pulmonary Medicine, University of Massachusetts Medical School, Worcester, MA 01655, USA; [2]Department of Pediatrics, University of Massachusetts Medical School, Worcester, MA 01655, USA; [3]Horae Gene Therapy Center, University of Massachusetts Medical School, Worcester, MA 01655, USA; [4]Department of Neurology, University of Massachusetts Medical School, Worcester, MA 01655, USA; [5]Department of Pediatrics, Duke University, Durham, NC 27710, USA

Amyotrophic lateral sclerosis (ALS) is a fatal neurodegenerative disease that results in death from respiratory failure. No cure exists for this devastating disease, but therapy that directly targets the respiratory system has the potential to prolong survival and improve quality of life in some cases of ALS. The objective of this study was to enhance breathing and prolong survival by suppressing superoxide dismutase 1 (SOD1) expression in respiratory motor neurons using adeno-associated virus (AAV) expressing an artificial microRNA targeting the SOD1 gene. AAV-miR^{SOD1} was injected in the tongue and intrapleural space of SOD1^{G93A} mice, and repetitive respiratory and behavioral measurements were performed until the end stage. Robust silencing of SOD1 was observed in the diaphragm and tongue as well as systemically. Silencing of SOD1 prolonged survival by approximately 50 days, and it delayed weight loss and limb weakness in treated animals compared to untreated controls. Histologically, there was preservation of the neuromuscular junctions in the diaphragm as well as the number of axons in the phrenic and hypoglossal nerves. Although SOD1 suppression improved breathing and prolonged survival, it did not ameliorate the restrictive lung phenotype. Suppression of SOD1 expression in motor neurons that underlie respiratory function prolongs survival and enhances breathing until the end stage in SOD1^{G93A} ALS mice.

INTRODUCTION

Amyotrophic lateral sclerosis (ALS) is a devastating, untreatable neurodegenerative disease. Patients with ALS die 3–5 years after diagnosis from respiratory failure, and death is accelerated if the bulbar muscles and motor neurons are affected early in the disease.[1] Bulbar involvement leads to recurrent aspiration, choking, and aggravation of respiratory disease.[2,3] The most severely affected bulbar muscle is the tongue,[4] which atrophies as a result of loss of the hypoglossal motor neurons and neuromuscular junction (NMJ) disruption.[5–7] In addition to tongue involvement, all individuals afflicted with ALS develop progressive diaphragm and intercostal weakness that results in inadequate ventilation and respiratory failure.[8–10] As a result of the tongue and respiratory pathology, patients progressively develop decreased exercise tolerance, shortness of breath, early morning headaches, and excessive daytime sleepiness. The rate of decline in respiratory function is directly related to mortality.[11–13] Furthermore, respiratory support with non-invasive positive pressure ventilation significantly prolongs survival.[12,14]

Approximately 5%–10% of ALS is familial, and 20% of familial ALS is due to mutations in the gene encoding Cu/Zn superoxide dismutase 1 (SOD1).[15] The exact mechanism of the SOD1-induced neurotoxicity is unclear, but aggregations of mutant SOD1 result in a cascade of events that eventually leads to neuronal degeneration. The SOD1^{G93A} mouse is the most commonly used ALS mouse model. It ubiquitously expresses the human SOD1 gene with the G93A mutation[16] and recapitulates ALS pathophysiology, including motor neuron loss, axonal degeneration, muscle denervation, and limb paralysis.[16–18] In addition, this mouse model has significant respiratory insufficiency, restrictive lung disease, and hypoventilation.[18] Furthermore, the SOD1^{G93A} mouse has orolingual motor deficits that initially appear as tongue motility abnormalities and then progress to tongue force weakness.[19–21] This pathology significantly impacts breathing because the tongue genioglossal muscle contracts during breathing and maintains upper airway patency in the face of the negative intrathoracic pressure that occurs with each breath.

There is no cure for ALS. Novel therapies aimed at silencing SOD1 include inhibitory short hairpin RNA, artificial microRNA (miRNA), and anti-sense oligonucleotides. Our group recently reported successful silencing of SOD1 in mice and non-human primates using adeno-associated virus (AAV) gene therapy encoding a miRNA (AAV-miR^{SOD1}).[22–24] When injected into neonatal mice, survival was prolonged by 69 days,[22] whereas a systemic injection in adult mice resulted in extension of lifespan by 22–27 days.[23] Despite this systemic therapy, respiratory insufficiency persisted.[22,23] We hypothesized that these animals eventually died of respiratory failure.

Received 25 July 2019; accepted 13 December 2019;
https://doi.org/10.1016/j.omtm.2019.12.007.

Correspondence: Christian Mueller, Department of Pediatrics, University of Massachusetts Medical School, Worcester, MA 01655, USA.
E-mail: chris.mueller@umassmed.edu
Correspondence: Mai K. ElMallah, Division of Pulmonary Medicine, Department of Pediatrics, Duke University, Durham, NC 27710, USA.
E-mail: mai.elmallah@duke.edu

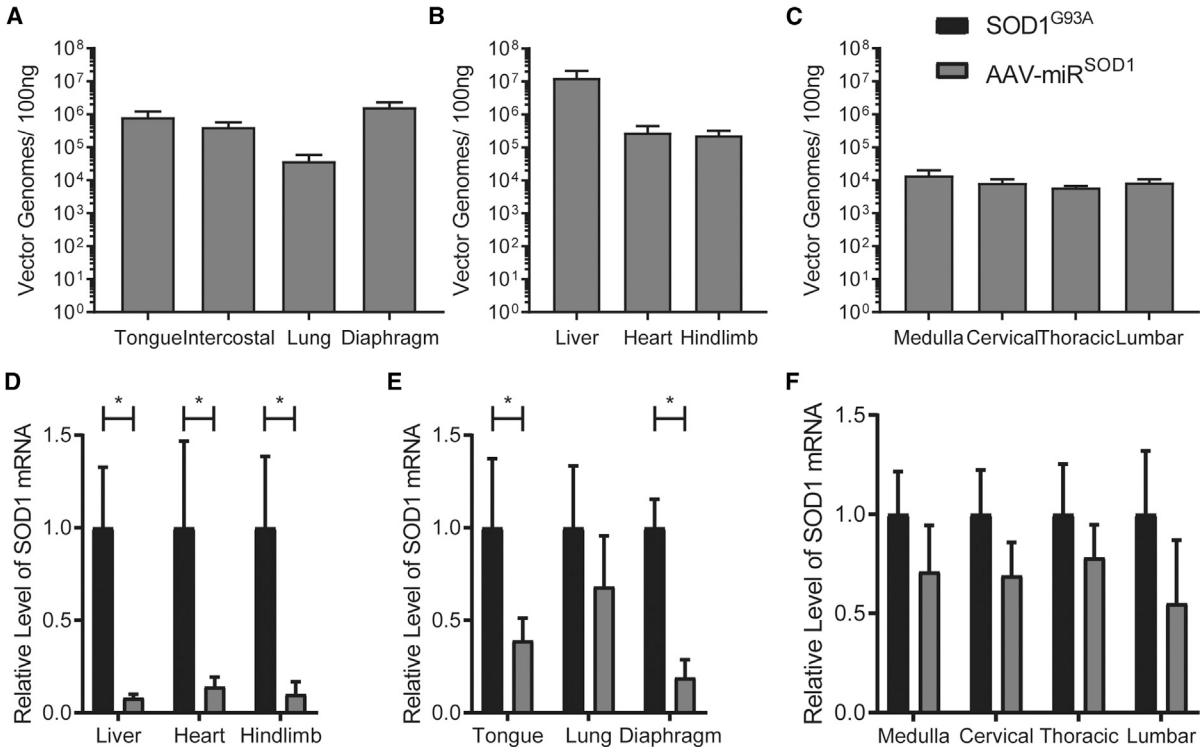

Figure 1. Intralingual and Intrathoracic Injections of AAV-miR^{SOD1} Are Systemically Distributed and Lead to Widespread Suppression of SOD1 Expression
(A–F) Quantitative PCR estimates of vector genomes are shown in (A) peripheral tissues (liver, heart, hindlimb), (B) respiratory muscles, and (C) four regions of the CNS. qRT-PCR estimates of levels of SOD1 mRNA are illustrated for extracted (D) peripheral tissues (liver, heart, hindlimb), (E) respiratory muscles, and (F) four regions of the CNS. Error bars represent ± standard error of the mean (SEM) (A–C) and ± positive and negative error (D–F). n = 4, Student's *t* test to determine significance in (D)–(F) comparing untreated to treated. *p < 0.005.

Therefore, the goal of this study was to evaluate the impact of gene-silencing therapy targeted to respiratory motor units on breathing and survival, with the ultimate goal of using this as an adjunct therapy to systemic or intrathecal delivery. Since respiratory support in ALS patients prolongs survival, we hypothesized that suppression of SOD1 expression in motor neurons that underlie respiration would prolong survival. We used a combination of intralingual (specifically genioglossal) and intrapleural AAV-miR^{SOD1} injections exploiting intramuscular delivery and retrograde axonal transport to target the entire motor unit: muscle, NMJ, motor axon, and motor neurons. The tongue genioglossal delivery targets both the muscle and hypoglossal motor neurons,[25,26] while intrathoracic delivery targets the diaphragm and intercostal muscles as well as the phrenic and thoracic motor neurons.[27] Our ultimate goal was to reduce expression of the mutant SOD1 in the tongue and respiratory motor units and thereby enhance breathing and prolong survival.

RESULTS

To assess the benefit of respiratory-targeted gene therapy for ALS, we injected the SOD1^{G93A} mutant mouse model with 1×10^{11} vector genomes (vg) via an intralingual injection and 1×10^{11} vg via an intrapleural injection of AAVrh.10 encoding an artificial microRNA targeting *SOD1* (AAV-miR^{SOD1}). SOD1^{G93A} animals were injected as adults at approximately 60 days of age with the therapeutic vector, AAV-miR^{SOD1}, or saline, and non-transgenic littermate animals were used as additional controls. All animals were followed longitudinally until they were not able to right themselves within 30 s after being placed on either side.

Respiratory-Directed Therapy Results in Efficient Muscle and CNS Transduction as well as SOD1 mRNA Levels Silencing

To assess the level of transduction and *SOD1* mRNA silencing, we evaluated vector genome expression in treated SOD1^{G93A} mice. Efficient targeting of the AAV-miR^{SOD1} vector was observed in the tongue, intercostal muscles, lung, and diaphragm (Figure 1A). To assess the extent of systemic distribution, we examined vector genome levels in the liver, heart, and hindlimb. Injections targeting the tongue and thoracic cavity led to a considerable amount of vector genomes in the liver, heart, and hindlimb (Figure 1B). Vector genomes were also detected in the medulla and throughout the entire spinal cord (Figure 1C). To assess retrograde transport to the hypoglossal nucleus and phrenic motor nucleus by intralingual and intrathoracic injections, we injected SOD1^{G93A} mice with an AAVrh10 vector containing GFP. At the end stage in the SOD1^{G93A}

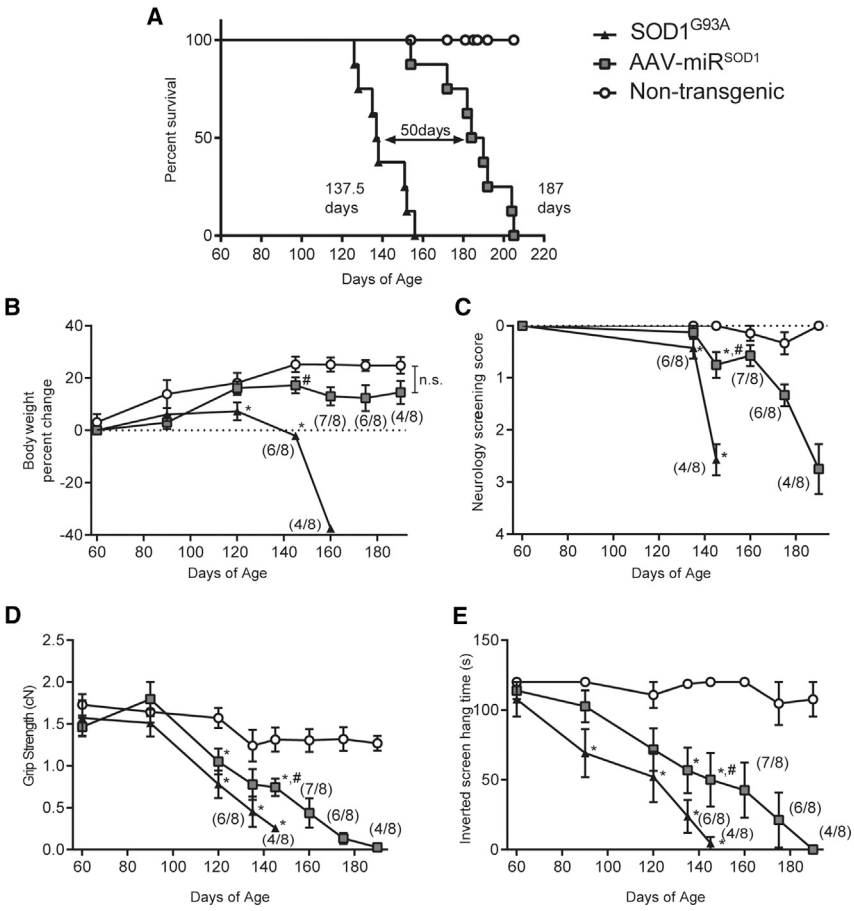

Figure 2. AAV-miR^{SOD1}-Treated Animals Show Increased Survival and Improved Maintenance of Weight and Strength

(A) A Kaplan-Meier percent survival plot documents an increase in 36% cumulative survival of 50 days in AAV-mir^{SOD1} mice. Survival logrank (Mantel-Cox) test, $p < 0.0001$. (B) Percent change in body weight plotted from day 60 until endpoint. (C) Changes in the neurological screening from day 60 to endpoint. This ranges from 0 (the mouse appears normal) to 4 (the mouse cannot right itself within 30 s of being placed on either side). (D) Four-limb grip strength measured in centinewtons (cN). (E) Inverted screen hanging test time, plotted to a maximum of 120 s. With the exception of (A), data are represented as mean ± SEM; a one-way ANOVA was performed for each time point, $p < 0.05$. Multiple comparisons between groups were performed using the Fisher's least significant difference (LSD) test. N = 8 at start of experiment; N/8 is listed for each time point for SOD1- and mir-treated animals. For non-transgenics (NTGs), n was the following at each time point (not from humane endpoint but for age-matched controls): 160 days, n = 7; 175 days, n = 6; 190 days, n = 3. *$p < 0.05$, significantly different from NTG littermates; $^{\#}p < 0.05$, significantly different from untreated SOD1.

mice we observed GFP staining of motor neurons in the hypoglossal motor nucleus and phrenic motor nucleus, respectively (Figure S1).

Next, we evaluated mRNA expression levels in treated and untreated SOD1^{G93A} mice. Transduction within the tongue and respiratory muscles led to robust silencing of *SOD1* mRNA by 64% in the tongue and 80% in the diaphragm (Figure 1D).The lung had a more modest reduction of *SOD1* mRNA (35%). Efficient silencing was also observed systemically, as evidenced by a decrease in expression by 86%, 87%. and 89%, in the liver, heart, and hindlimb, respectively (Figure 1E). Suppression of *SOD1* mRNA was also observed in the medulla and spinal cord ranging from 23% to 45% (Figure 1F).

Delayed Disease Onset and Prolonged Survival in AAV-miR^{SOD1}-Treated SOD1 Mice

Animal strength and behavior were assessed every 30 days until disease onset and then every week thereafter. AAV-miR^{SOD1} therapy targeting the respiratory system significantly enhanced survival by an average of 50 days in treated compared to untreated SOD1^{G93A} mice (Figure 2A). Weight loss, neurological symptoms, and muscle strength were also assessed. A significant improvement in weight gain was observed in treated compared to untreated SOD1^{G93A} mice, with some treated mice maintaining weight until 190 days of life (Figure 2B). Neurological screening using a standard ALS neurological screening metric[28] revealed that, compared to untreated SOD1^{G93A} mice, AAV-miR^{SOD1}-treated SOD1^{G93A} mice had a slower neurological decline (Figure 2C). A four-limb grip strength test (Figure 2D) and inverted screen testing (Figure 2E) revealed less rapid deterioration of muscle strength in AAV-miR^{SOD1}-treated mice compared to untreated SOD1^{G93A} mice. Overall, AAV-miR^{SOD1}-treated SOD1^{G93A} mice showed enhanced survival, weight gain, and neurological improvement.

Enhancement of Breathing in AAV-miR^{SOD1}-Treated SOD1^{G93A} Mice

Whole-body plethysmography (WBP) was used to assess the therapeutic benefits of tongue and respiratory-directed AAV-miR^{SOD1} on respiratory function. WBP measures frequency, lung volumes, and flow rates in awake spontaneously breathing animals. At 90 days and 130–149 days, no significant differences in breathing parameters were observed between the treated and untreated SOD1^{G93A} mice or between the SOD1^{G93A} and non-transgenic littermates (Figures 3A–3E). At the final time point from 150 to 169 days, few untreated animals remained (n = 2) and they had a decreased respiratory rate (frequency) compared to the remaining AAV-miR^{SOD1}-treated SOD1^{G93A} mice (n = 8) (Figure 3A). In addition, the untreated SOD1^{G93A} mice had decreased tidal volumes compared to non-transgenic littermates (Figure 3B) and decreased minute ventilation (Figure 3C) compared to both the

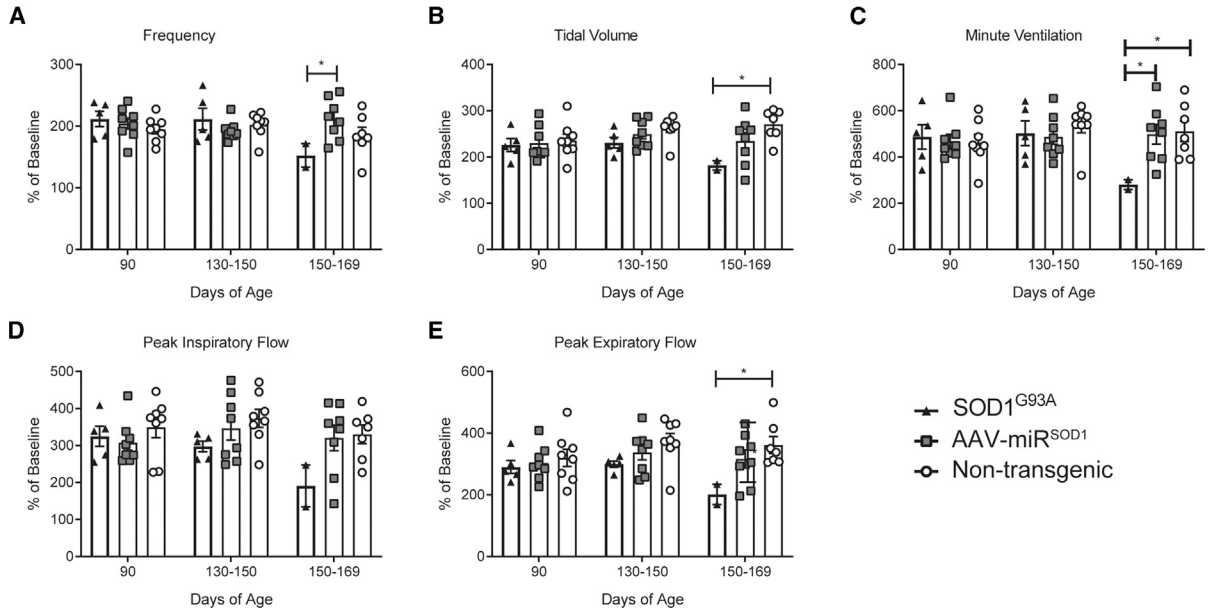

Figure 3. AAV-miR^{SOD1} Animals Display Improvement in Breathing

Whole-body plethysmography of awake spontaneously breathing animals. Data are reported as a percentage of response to a 10-min period of hypercapnia compared to baseline breathing. (A and B) At the untreated SOD1^{G93A} endpoint (151–169 days), significant differences are noted between AAV-miR^{SOD1} in (A) frequency and NTG littermates in (B) tidal volume. (C) Minute ventilation findings for both treated and NTG littermates were significantly different from untreated animals at the untreated SOD1 endpoint. (D and E) No differences were observed in (D) peak inspiratory flow between any group, but significant differences were noted between NTG littermates and untreated animals in (E) peak expiratory flow. All data are represented as mean ± SEM. Starting numbers were n = 8 for AAV-miR^{SOD1}, n = 5 for untreated SOD1^{G93A}, and n = 8 for NTG. Only two untreated animals survived to the day 150–169 time point. A mixed-effects model was used to take into account missing animals that did not survive to the later time points. Multiple comparisons between groups were performed using the Fisher's LSD test. *$p < 0.05$.

AAV-miR^{SOD}-treated SOD1^{G93A} mice and the non-transgenic littermates (for both). Untreated SOD1 mice had decreased peak expiratory flow (PEF) and decreased peak inspiratory flow (PIF) compared to non-transgenic littermates, suggesting increased weakness in respiratory muscles (Figure 3E). Furthermore, compared to the AAV-miR^{SOD1}-treated SOD1^{G93A} mice, the untreated mice had decreased PIF and PEF. PIF and PEF reflect inspiratory muscle strength and expiratory muscle strength, respectively. Thus, the AAV-miR^{SOD1}-treated SOD1^{G93A} mice behaved similarly to non-transgenic littermates, in that they survived to this time point and maintained respiratory muscle strength, frequency, tidal volume, and minute ventilation. Thus, overall breathing decline was attenuated in the SOD1^{G93A} mice treated with AAV-miR^{SOD1}, whereas surviving untreated SOD1^{G93A} mice had declines in several respiratory parameters.

To assess the pulmonary mechanics of AAV-miR^{SOD1}-treated animals, forced oscillometry techniques were used at disease endpoint. The total respiratory resistance, central airway resistance, and tissue resistance were all increased in both the AAV-miR^{SOD1}-treated and untreated SOD1^{G93A} animals (Figures S2A–S2C). Similarly, the inspiratory capacity and respiratory compliance were decreased at endpoint in both untreated and AAV-miR^{SOD1}-treated animals. Thus, no significant improvement occurs in pulmonary mechanics in either untreated or treated SOD1^{G93A} mice.

Preservation of Motor Neurons and Corresponding Peripheral Synaptic Terminals

The impact of therapy on motor neuron survival was examined using histological quantification. Specifically, we quantified cresyl violet-stained hypoglossal and cervical ventral motor neurons at the endpoint (Figure 4). Non-transgenic littermates had significantly more motor neurons in both hypoglossal and cervical ventral regions than both the untreated or treated animals did, suggesting that at disease endpoint motor neuron death was similar between treated and untreated animals.

To assess the effect of respiratory-directed therapy on axonal integrity of hypoglossal and the phrenic nerve, these were collected from animals at the endpoint, with non-transgenic littermates being age matched to the treated group (Figure 5). In the AAV-miR^{SOD1}-treated mice, there was a preservation of axonal numbers at the end stage in the hypoglossal and phrenic nerves. However, despite the preservation of axon numbers, the size of the axons was significantly smaller (Figure 5D).

To assess the impact of distal nerve degeneration, we assayed the NMJs in the tongue and diaphragm at the endpoint. Within the diaphragm, the untreated animals revealed significant disruption of the NMJs (Figure 6). In contrast, in the AAV-miR^{SOD1}-treated diaphragm, there was some preservation of presynaptic and postsynaptic components of the

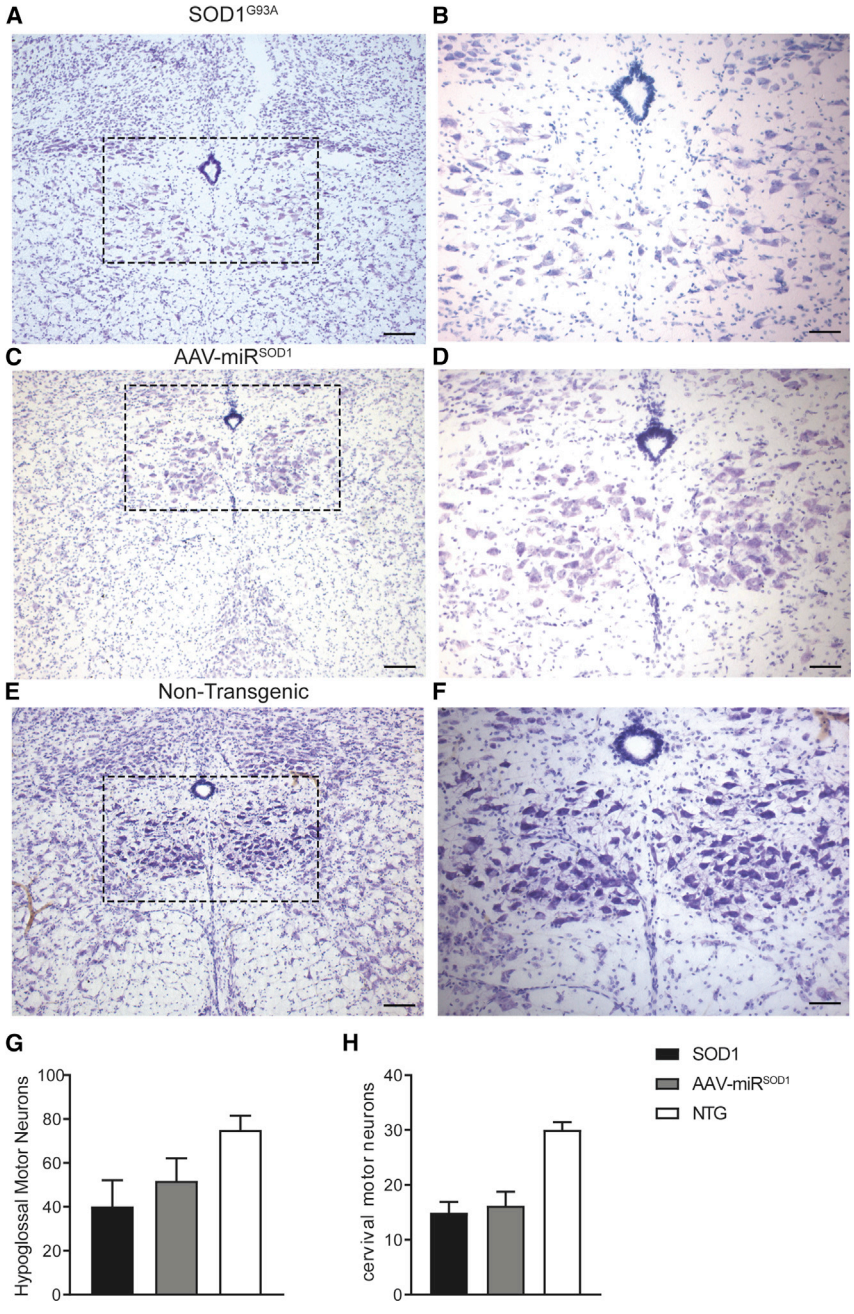

Figure 4. Motor Neuron Death Is Observed in Both Treated and Untreated SOD1 Animals

Representative images of cresyl violet staining for motor neurons within the hypoglossal nuclei were stained from tissues harvested at their respective endpoints: (A) untreated SOD1^{G93A} animals (137 days), (C) AAV-miR^{SOD1}-treated SOD1^{G93A} mice (190 days), and (E) NTG littermate controls (192 days). (B), (D), and (F) are higher magnifications of the boxed area in panels (A), (C), and (E), respectively. Scale bars for (A), (C), and (E), 100 μm; for (B), (D), and (F), 50 μm. (G and H) Motor neuron quantification: (G) hypoglossal motor neuros, (H) cervical motor neurons. All data are represented as mean ± SEM. n = 4 for AAV-miR^{SOD1}, n = 3 for untreated SOD1^{G93A}, and n = 6 for NTG (n = 5 for phrenic). A one-way ANOVA was performed with uncorrected Fisher's LSD multiple comparisons test. *p < 0.05

NMJ (Figure 6). Within the tongue of the untreated animals there was significant denervation of NMJs (Figure S3). AAV-miR^{SOD1} treatment mitigated this denervation, but this improvement was not as robust as in the diaphragm (Figure 6; Figure S3).

DISCUSSION

The most significant outcome of this study is that targeting respiratory motor neurons using AAVrh.10 expressing an artificial miRNA against the SOD1 (AAV-miR^{SOD1}) significantly prolongs survival in adult SOD1^{G93A} ALS mice. In addition, respiratory function was preserved until end stage disease and disease onset was delayed. This study highlights the importance of treating the respiratory system in ALS.

AAV Gene Therapy for ALS

It is difficult to directly compare AAV gene therapy animal studies because of variations in injection routes, capsid variants, vector constructs and genomes, titration methods of different laboratories, vector dosages, and age of animals when treated. However, similar studies using different routes of injection have been performed in SOD1 mouse models with varying results. Recent studies from our group documented that an SOD1-targeting miRNA delivered by AAV9 prolongs survival by ~70 days in SOD1^{G93A} mice when injected in the neonatal period.[22] In a more direct comparison, our group used the same capsid and similar vector, AAVrh.10-mir SOD1, intravenously in adult mice and survival was only prolonged by 22–27 days.[23] Similarly, a recent study using AAVrh10 to express a small nuclear RNA that skips exon 2 out of frame reported significant improvement in survival in mice treated at both adult and neonatal ages.[29] In a subset of mice, limb function was completely preserved in their study, comparable to our earlier observation.[22] In addition, other groups used AAV2 or AAV9 to deliver therapeutic genes, such as insulin growth factor 1 (IGF-1)[30–33] into muscles, including the muscles of respiration. The goal of both of these studies was to use retrograde transport of AAV to transduce the motor neurons of interest.[30,32] Both studies saw significant enhancement in survival at ~30–37 days when the muscles of respiration, such as the intercostal muscles, were targeted versus ~10–12 days without intercostal muscle injections.[30,32]

AAVrh10 was an ideal choice for this present study because of its ability to cross the blood-brain barrier and to transduce motor neurons by retrograde transport.[34,35] In addition, AAVrh10 is safe and efficacious in both mice and non-human primate models.[23,24] The utility of AAVrh10 is underscored by proof-of-principle and safety data generated with this vector design in cynomolgus macaques.[24] In our current study, we injected 2×10^{11} vg of AAV expressing the miR^{SOD1}, which is 1/10th of the dose that was injected systemically (see Borel et al.[24]) or 1/39th of the dose co-injected intracerebroventricularly and systemically in adult mice (see Biferi et al.[29]), and we report an improvement in survival by 50 days, whereas other reported 22–27 days and 63 days, respectively.

Respiratory Involvement in ALS

All individuals afflicted with ALS ultimately succumb to inadequate ventilation and respiratory failure secondary to diaphragm and intercostal muscle weakness.[8–10] These muscles are essential for breathing and are innervated by the phrenic nerve in the ventral horn of C3–C5 and by the intercostal motor neurons in T1–T12 in the thoracic spinal cord. The largest increase in lifespan to date in an SOD1 mouse model was reported in a study that also targeted the respiratory muscles. Specifically, this study used a lentiviral short hairpin RNA (shRNA) delivered by a series of intramuscular injections that included hindlimb, facial, tongue, diaphragm, and intercostal muscles.[36] Through an intralingual and intrapleural injection of AAV gene therapy, our goal was to target the entire motor unit of the tongue, diaphragm, and intercostal muscles. Specifically, we sought to target the nerves and motor neurons innervating these muscles. Using the AAVrh10-GFP we found positive GFP staining in the phrenic and hypoglossal motor nuclei (Figure S1). In addition, at the end stage in AAV-miR^{SOD1}-treated animals, we report improvements in NMJ in the diaphragm, and preservation of axonal integrity of the phrenic nerve, but the survival of the hypoglossal and cervical ventral motor neurons was not significantly different. Treated animals showed evidence of greater respiratory muscle strength as seen with preserved PIF and PEF. However, motor neuron loss and restrictive lung disease were still evident at the end stage. We previously reported restrictive lung disease in SOD1^{G93A} mice.[18] Unfortunately, AAV-miR^{SOD1} therapy targeting the respiratory system did not prevent restrictive lung disease, and at the end stage mice succumbed to respiratory failure. A recent report utilizing muscle-specific kinase (MuSK) antibody therapy preserved NMJs in the diaphragm but did not improve diaphragm strength or breathing.[37] This suggests the importance of not only preserving the NMJ but also the motor neurons. The eventual decline in respiratory function and restrictive lung disease may be caused by inefficient targeting of all neuronal cells present in the motor nuclei innervating the diaphragm and intercostal muscles. Thus, combining respiratory directed and intravenous, intracerebral ventricle, or intrathecal infusion may be necessary to treat all neuronal cells affected. Since positive pressure ventilation enhances survival and quality of life, combination therapy has the ability to treat respiratory insufficiency and enhance survival and quality of life.

Tongue Involvement in ALS

Patients with ALS who initially present with bulbar symptoms have a worse prognosis and rapidly progressive disease course.[1] The most severely affected bulbar muscle is the tongue.[4] These abnormalities of the tongue are a result of atrophy due to loss of the hypoglossal motor neurons,[7] which control the intrinsic and most extrinsic muscles of the tongue.[6]

The hypoglossal motor neurons are also important in maintaining upper airway patency, as these cells regulate the shape, stiffness, and position of the tongue.[6,38–40] Contraction of the extrinsic tongue muscles dilate and stiffen the pharyngeal lumen and prevent collapse in the face of negative inspiratory pressures.[41,42] Thus, degeneration of hypoglossal motor neurons in ALS results in upper airway obstruction, oral phase dysphagia, and recurrent aspiration. With our dual injection strategy, we were able to significantly silence expression of SOD1 within the tongue. Interestingly, this tongue correction correlated with maintenance of weight and increased survival in treated animals.

Although our approach targeted the respiratory system, it is important to note that we did see systemic distribution of virus that was correlated with significant reduction in SOD1 mRNA expression in the liver, heart, and limb skeletal muscle. We think that the systemic distribution of vectors in combination with the directed lingual treatment enhanced survival in these animals. Thus, we propose that future gene therapy approaches should consider a dual injection (systemic and intralingual or intrathecal and intralingual) to ensure that the hypoglossal motor neurons are targeted. If successful, we think that this will allow patients better control of their tongue, maintenance of upper airway patency, and decreased aspiration of secretion.

In conclusion, this study illustrates the importance of targeting the respiratory system in the treatment of ALS. Ideally, a therapy would target the entire CNS with focus on both motor units responsible for respiration and ambulation. However, our directed approach clearly demonstrates the degree to which respiratory rescue can enhance survival. In addition, a robust improvement in survival in adult animals was documented at considerably lower doses than previously published. Correction of hindlimb paralysis is an important functional benchmark in treated ALS, and indeed we saw modest but significant improvement in limb strength in our study. However, because respiratory failure is the ultimate cause of death in this disease, future therapeutics should also target the respiratory system.

MATERIALS AND METHODS

Animals

All experimental procedures were approved by the Institutional Animal Care and Use Committee at the University of Massachusetts Medical School. SOD1^{G93A} animals were randomly assigned to the AAVrh10-H1-miR^{SOD1} (n = 8, 7 females, 1 male) versus the phosphate-buffered saline (PBS) group (N = 8, 6 females, 1 male). Littermate non-transgenic controls (n = 8, 7 females, 1 male) were injected with PBS. Injections were administered by an investigator blinded to the groups. Mice transgene copy numbers were monitored by quantitative

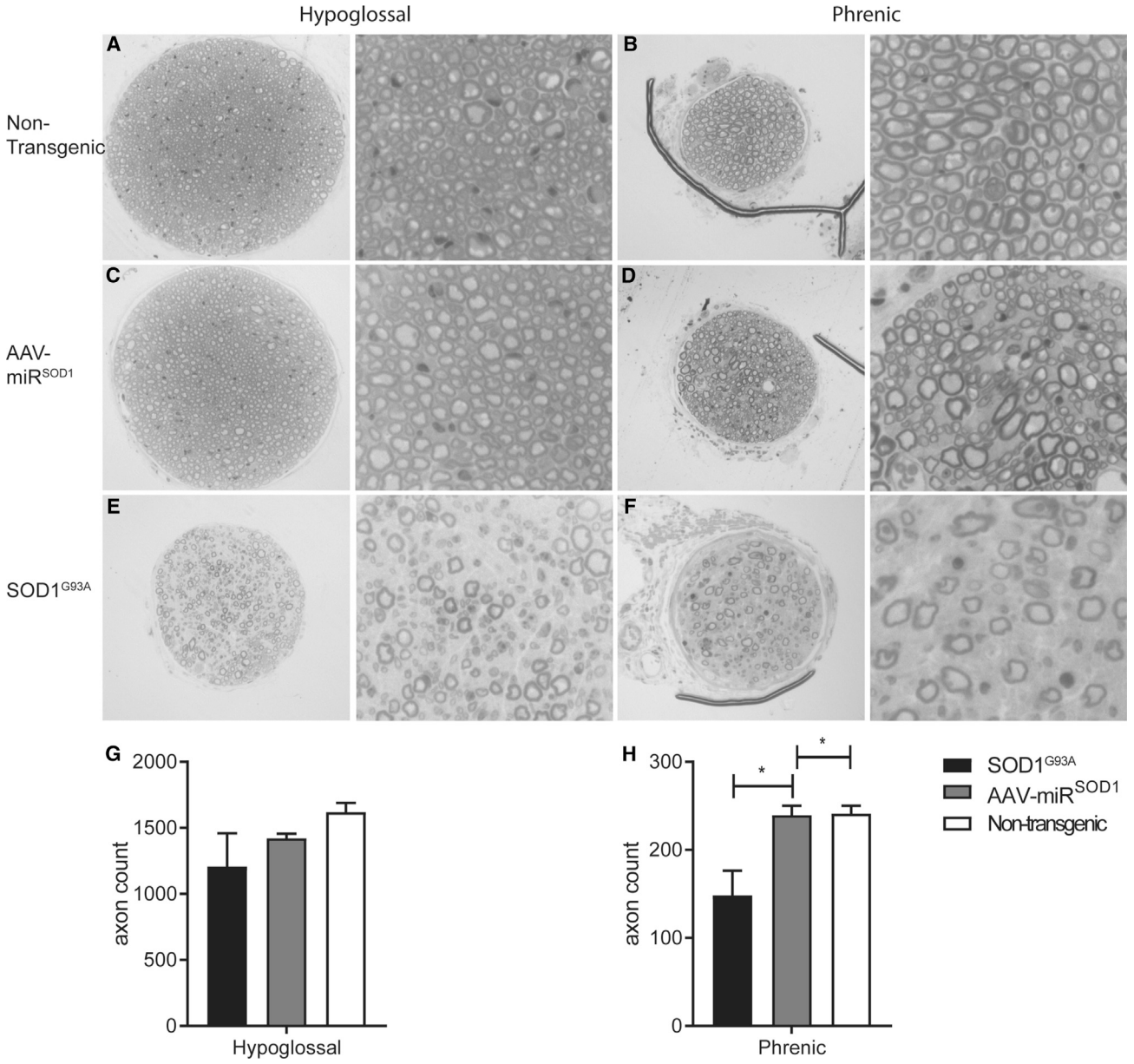

Figure 5. AAVmiR^{SOD1} Preserves Axons within the Hypoglossal and Phrenic Nerves

(A–F) Representative cross-sections of hypoglossal (A, C, and E) and phrenic (B, D, and F) nerves stained with toluidine blue at endpoint for treated and untreated SOD1^{G93A} mice at their respective endpoints and age-matched NTG littermate controls. NTG littermate (172 days) (A and B), AAV-mir^{SOD1} (190 days) (C and D), and untreated (156 days) (E and F). (G and H) Quantification of axons was performed within the hypoglossal (G) and phrenic (H) nerves. All data are represented as mean ± SEM. n = 3 for all groups; one-way ANOVA was performed with an uncorrected Fisher's LSD multiple comparisons test. *$p < 0.05$.

real-time-PCR according to Prize for Life and Jackson Laboratory guidelines such that any mice with fewer than 20 copies or more than 25 copies were excluded.

AAV Vectors and Injection Methods

AAVrh10-H1-miR^{SOD1} vectors (hereafter AAV-miR^{SOD1}), targeting the human SOD1 sequence, were generated as described.[23,24] The vector construct contains mutated inverted terminal repeats (ITRs) to create dsAAV vectors, a single miR sequence driven by the H1 promoter, and a rabbit poly-globin poly(A) tail (clinical H1 construct described in Borel et al.[24]). All vector doses were per animal, at 1×10^{11} vg or PBS, and they were injected into each location at a volume of 40 μL in the tongue and 400 μL in the intrapleural space described for a total vector dosage of 2×10^{11} vg per animal.[25–27]

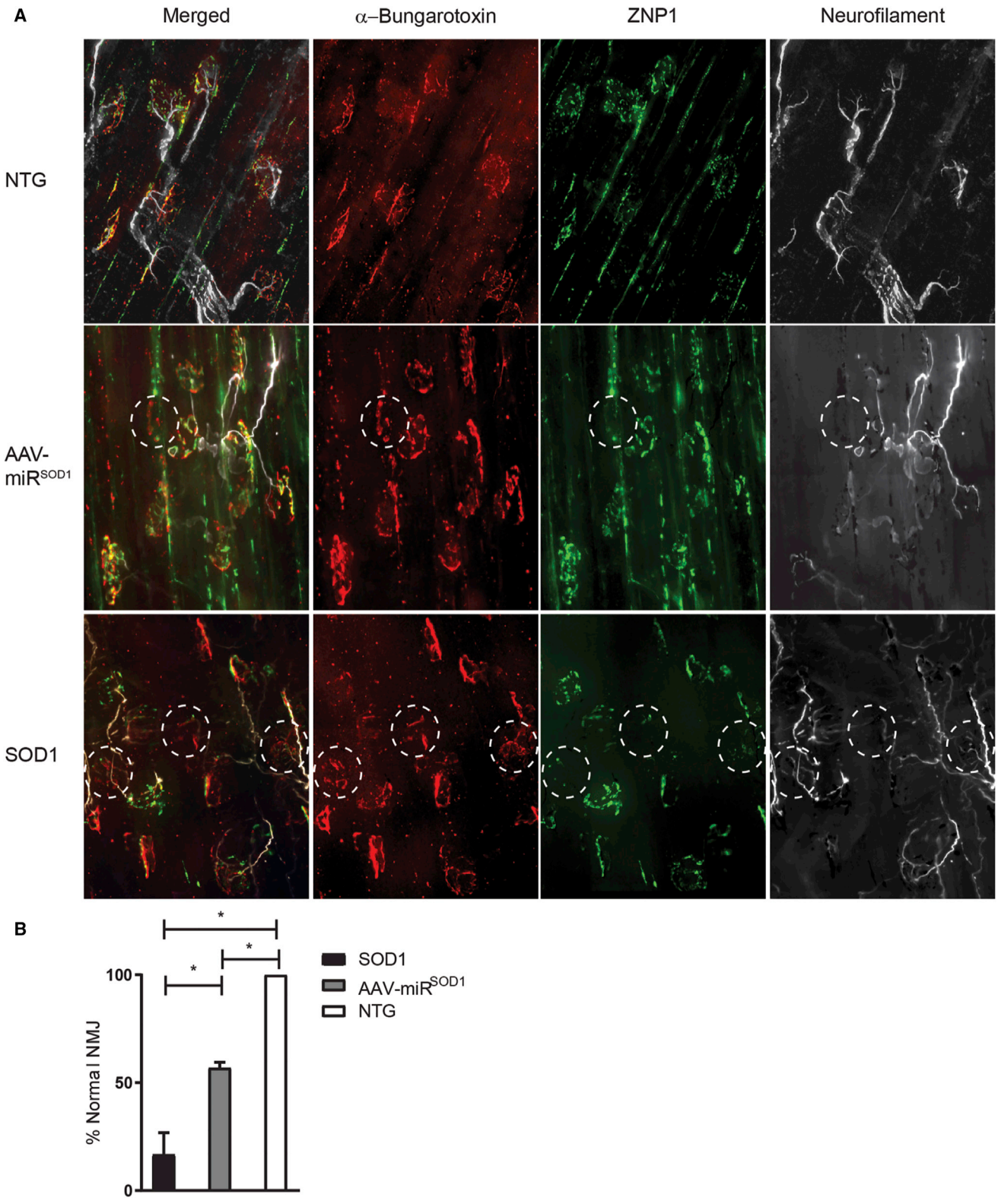

(legend on next page)

Injections were performed by an investigator blinded to the groups and the study drug. The intralingual injections were performed as previously described,[25] and the intrapleural injections were performed as previously described.[27] SOD1^{G93A} animals were injected at approximately 60 days of age with either AAV-miR^{SOD1} or PBS, and non-transgenic littermates were used as additional controls. All animals were followed longitudinally.

Behavior Testing

Four-limb grip strength and inverted screen testing were determined by a an investigator blinded to the experimental groups, as previously described.[43] The four-limb grip strength test was performed using mesh screen on an Alemno digital grip strength meter (Holzkirchen, Germany) to determine peak force. Each grip test was repeated twice with a 15-min rest period, and the maximum force was recorded. An inverted screen was performed using square wire mesh rotated 180°. Animals were assessed for latency to fall up to 2 min, and again this was repeated twice per session with a 15-min rest period, and the longest hang time was recorded. For the neurological screening score assessment, an investigator blinded to groups scored animals according to Prize for Life and Jackson Laboratory guidelines based on the following: 0, full extension of hind legs from midline when suspended by tail; 1, collapse of leg extension toward midline or trembling; 2, toes curl under at least twice when walking or any foot dragging; 3, paralysis or minimal joint movement; and 4, mouse cannot right itself within 30 s after being placed on either side.

Ventilation

Ventilation was quantified using whole-body plethysmography in unrestrained, unanesthetized mice as previously described.[18,43] Awake, non-restrained mice were placed inside a 3.5 × 5.75-in Plexiglas chamber (SCIREQ, Montreal, QC, Canada) and data were collected in 10-s intervals. The Drorbaugh and Fenn[44] equation was used to calculate respiratory volumes, including tidal volume and minute ventilation. Mice immediately underwent a 10-min hypercapnic challenge (fraction of inspired O_2 [FiO_2], 0.21; fraction of inspired CO_2 [$FiCO_2$], 0.07; nitrogen balance) followed by a subsequent 60- to 90-min eupnea period when they were exposed to normoxic air (FiO_2, 0.21; nitrogen balance).

Measures of Pulmonary Mechanics

Pulmonary mechanics were performed at the study endpoint using forced oscillometry (FlexiVent system, SCIREQ, Montreal, QC, Canada) at baseline and in response to incremental doses of methacholine as previously described.[45] In brief, animals were anesthetized with an intraperitoneal (i.p.) injection of a mixture of ketamine (90 mg/kg, Animal Health International) and xylazine (4.5 mg/kg, Propharma), and a tracheotomy was performed followed by insertion of a pre-calibrated cannula into the trachea. Spontaneous respiratory effort was prevented using a neuromuscular blocking agent (pancuronium bromide, 2.5 mg/kg; Hospira, Lake Forest, IL, USA). Respiratory mechanics were obtained and calculated using FlexiWare software (SCIREQ, Montreal, QC, Canada) as previously described.[18,43,45,46]

Vector Genomes

Genomic DNA (gDNA) was extracted using a DNeasy blood and tissue kit (QIAGEN, Valencia, CA, USA) from the tissues harvested from AAV- and PBS-injected animals at the study endpoint.[43] Quantitative real-time PCR was carried out using custom TaqMan gene expression master mix (Applied Biosystems) and TaqMan probes (Applied Biosystems) for a custom probe against rabbit poly-globin poly(A) tail (probe, 5′-/56-FAM/ATGAAGCCCCTTGAGCATCT GACTTCT/36-TAMSp/-3′; primer 1, 5′-GCCAAAAATTATGGGG ACAT-3′; primer 2, 5′-ATTCCAACACACTATTGCAATG-3′) with a plasmid control standard curve.

Analysis of RNA Knockdown

RNA was isolated with TRIzol (Invitrogen) and a Direct-zol RNA MiniPrep kit (Zymogen), then transcribed into complementary DNA using the High-Capacity RNA-to-cDNA kit (Applied Biosystems). qRT-PCR was carried out using TaqMan gene expression master mix (Applied Biosystems) and TaqMan probes (Applied Biosystems) for human SOD1 (Hs00533490_m1), and mouse hypoxanthine-guanine phosphoribosyltransferase (Hprt; Mm01545399_m1) as normalization gene. Relative expression was calculated as described.[22]

Immunostaining for NMJs

The tongue samples were embedded in optimal cutting temperature (OCT) compound and frozen. 20-μm-thick sections were cut for the tongue and stained by immunohistochemistry. Briefly, the tissue was incubated with alpha-bungarotoxin (Alexa Fluor 594 conjugated, 1:1,000; Invitrogen, #B-13422) for 2 h at room temperature, washed in PBS, and then tissue was incubated at least 24 h in a mixer of the two primary antibodies against neurofilament (1:400, chicken polyclonal to neurofilament NF-H, immunoglobulin [Ig]Y; EnCor Biotechnology, #CPCA-NF-H) and synaptotagmin (1:200; ZNP1 synaptotagmin, Zebrafish International Research Center, znp-1 #090811). The following day, the tissue was washed in PBS, incubated in an anti-mouse Alexa Fluor 488 (1:200) and in anti-chicken Alexa Fluor 647 (1:1,000) secondary antibodies for at least 24 h. The sections were washed in PBS, covered with fluorescent mounting media, and coverslipped. Diaphragm was not sectioned and was immunostained using the same method, except the incubation time was extended to at least 72 h at 4°C.

Figure 6. AAVmiR^{SOD1} Preserves Neuromuscular Junctions within the Diaphragm

Neuromuscular junctions (NMJs) were analyzed in untreated SOD1^{G93A} and AAV-miR^{SOD1} mice at their respective endpoints and in age-matched NTG littermate controls. (A) Immunofluorescence staining with rhodamine-conjugated α-bungarotoxin (red), as well as antibodies against anti-synaptotagmin (ZNP-1) and neurofilament-200 (gray). Denervation of NMJs is depicted by dashed circles. Representative images for NTG littermate control (205 days), AAV-miR^{SOD1} (205 days), and untreated SOD1^{G93A} (137 days) are shown. (B) Quantification of percent innervated NMJs is depicted. All data are represented as mean ± SEM. n = 4 for AAV-miR^{SOD1} and untreated SOD1^{G93A}, and n = 5 for NTG. One-way ANOVA was performed with an uncorrected Fisher's LSD multiple comparisons test. *$p < 0.05$.

Quantification of NMJ Integrity

NMJs in tongue and diaphragm were imaged using z series maximized projection on a Leica DM5500B microscope equipped with a 40× oil objective and fluorescent camera. Randomly selected equal area images were used to evaluate integrity of presynaptic (immunolabeled with synaptotagmin and neurofilament) and postsynaptic (labeled with bungarotoxin) structural components of each NM junction found in the field using the "Count" function of the Adobe Photoshop software. At least 10 images of the diaphragm were analyzed for each animal (total number of animals with diaphragm NMJ quantification: n = 4 for $SOD1^{G93A}$, AAV-miR^{SOD1} n = 5 for non-transgenic; total number of animlas for tongue NMJ quantification: n = 4 for AAV-miR^{SOD1} and non-transgenic, n = 5 for $SOD1^{G93A}$). A "normal" NMJ unit was considered to have well-structured presynaptic and postsynaptic components defined by colocalization of axon terminals with fluorescently labeled acetylcholine receptors (AChRs). In contrast, incomplete, or denervated, NMJs have AChR clusters on muscle fibers that are not contacted by an axon, as observed as an absence of anti-neurofilament staining.[47,48]

Cresyl Violet Staining and Quantification

The medulla and cervical spinal cord tissues were extracted and postfixed by immersion in 4% paraformaldehyde for at least 48 h and then transferred to 30% sucrose for cryoprotection and until sinking and were embedded in OCT compound and frozen. 40-μm-thick medullar and cervical spinal cord sections were mounted on glass slides and stained with cresyl violet stain pre-warmed to 60°C and coverslipped with Permount mounting medium (Thermo Fisher Scientific, Hampton, NH, USA). Images were taken on a Leica DM5500B bright-field microscope. Every sixth section was counted for a total of approximately 16 sections from each region in each mouse. Obtained values were averaged across each experimental group of animals, and the average of motor neurons per each section was graphed.

Toluidine Blue Staining and Quantification of Axonal Numbers

The hypoglossal and phrenic nerves were fixed in 2.5% glutaraldehyde in 0.1 M sodium cacodylate buffer (pH 7.2) overnight at 4°C, postfixed in 1% osmium tetroxide in 0.1 M sodium cacodylate buffer, and then embedded in epoxy resin. Blocks were trimmed to orient the nerves in order to obtain precise 1.5-μm-thick cross-sections on a Leica Ultracut E ultramicrotome. To quantify the number of axons, sections were counterstained with toluidine blue and coverslipped with Permount mounting medium (Thermo Fisher Scientific, Hampton, NH, USA) without dehydration in ethanol and the use of xylene as described elsewhere[22]. Once dried completely, slides were coverslipped with Permount mounting medium (Thermo Fisher Scientific, Hampton, NH, USA) without dehydration in ethanol and the use of xylene. Images were taken on a Leica DM5500B bright-field microscope. The number of axons was manually quantified using PhotoShop software. At least three mice were analyzed per experimental group.

Statistical Analysis

All statistical analyses were performed using Prism software (version 7, GraphPad, La Jolla, CA, USA). Survival logrank (Mantel-Cox) test was performed for survival analysis between all four treatment groups. A two-way ANOVA was performed for weights, strength testing, and measures of respiratory mechanics. A mixed-effects model was used to take into account missing animals that did not survive to the later time points. Multiple comparisons between groups and comparisons to baselines were performed using the Fisher's least significant difference (LSD) test. For the vector genomes, analysis was performed using the Student's t test, and significance for the enzyme assay and ventilation data was determined by one-way ANOVA. Significance was considered at a p value <0.05.

SUPPLEMENTAL INFORMATION

Supplemental Information can be found online at https://doi.org/10.1016/j.omtm.2019.12.007.

AUTHOR CONTRIBUTIONS

Conceptualization: A.M.K. and M.K.E.; Methodology: A.M.K., M.K.E., R.H.B., and C.M.; Formal Analysis: A.M.K., L.P., and M.K.E.; Investigation: A.M.K., M.Z., C.S., and A.V.; Resources: R.H.B., C.M., and M.K.E.; Writing – Original Draft: A.M.K. and M.K.E.; Writing – Review & Editing: A.M.K., M.Z., C.M., R.H.B., and M.K.E.; Visualization: A.M.K.; Project Administration: A.M.K. and M.K.E.; Funding Acquisition: M.K.E.

CONFLICTS OF INTEREST

C.M. and R.H.B. are co-founders of Apic Bio. Apic Bio has licensed patents related to this work in which C.M. and R.H.B. are both inventors. The remaining authors declare no competing interests.

ACKNOWLEDGMENTS

This work was supported by NIH/NICHD grant K08 HD077040-01A1, NIH/NINDS grants 1R21NS098131-01 (to M.K.E.), P01 HL131471, and R01-NS08868 (to C.M.); and ALS FindingACure, ALS ONE, the Angel Fund, the Celluci Fund, Project ALS, the Rosenfeld Fund, and Target ALS (to R.H.B.).

REFERENCES

1. Rosen, A.D. (1978). Amyotrophic lateral sclerosis. Clinical features and prognosis. Arch. Neurol. *35*, 638–642.
2. Rowland, L.P., and Shneider, N.A. (2001). Amyotrophic lateral sclerosis. N. Engl. J. Med. *344*, 1688–1700.
3. Forbes, R.B., Colville, S., and Swingler, R.J.; Scottish Motor Neurone Disease Research Group (2004). Frequency, timing and outcome of gastrostomy tubes for amyotrophic lateral sclerosis/motor neurone disease—a record linkage study from the Scottish Motor Neurone Disease Register. J. Neurol. *251*, 813–817.
4. Cha, C.H., and Patten, B.M. (1989). Amyotrophic lateral sclerosis: abnormalities of the tongue on magnetic resonance imaging. Ann. Neurol. *25*, 468–472.
5. DePaul, R., Abbs, J.H., Caligiuri, M., Gracco, V.L., and Brooks, B.R. (1988). Hypoglossal, trigeminal, and facial motoneuron involvement in amyotrophic lateral sclerosis. Neurology *38*, 281–283.
6. Fregosi, R.F., and Fuller, D.D. (1997). Respiratory-related control of extrinsic tongue muscle activity. Respir. Physiol. *110*, 295–306.
7. Ferrucci, M., Spalloni, A., Bartalucci, A., Cantafora, E., Fulceri, F., Nutini, M., Longone, P., Paparelli, A., and Fornai, F. (2010). A systematic study of brainstem motor nuclei in a mouse model of ALS, the effects of lithium. Neurobiol. Dis. *37*, 370–383.

8. Schiffman, P.L., and Belsh, J.M. (1993). Pulmonary function at diagnosis of amyotrophic lateral sclerosis. Rate of deterioration. Chest *103*, 508–513.

9. Ilzecka, J., Stelmasiak, Z., and Balicka, G. (2003). Respiratory function in amyotrophic lateral sclerosis. Neurol. Sci *24*, 288–289.

10. Ahmed, R.M., Newcombe, R.E., Piper, A.J., Lewis, S.J., Yee, B.J., Kiernan, M.C., and Grunstein, R.R. (2016). Sleep disorders and respiratory function in amyotrophic lateral sclerosis. Sleep Med. Rev. *26*, 33–42.

11. Fallat, R.J., Jewitt, B., Bass, M., Kamm, B., and Norris, F.H., Jr. (1979). Spirometry in amyotrophic lateral sclerosis. Arch. Neurol. *36*, 74–80.

12. Kleopa, K.A., Sherman, M., Neal, B., Romano, G.J., and Heiman-Patterson, T. (1999). Bipap improves survival and rate of pulmonary function decline in patients with ALS. J. Neurol. Sci. *164*, 82–88.

13. Leonardis, L., Dolenc Groselj, L., and Vidmar, G. (2012). Factors related to respiration influencing survival and respiratory function in patients with amyotrophic lateral sclerosis: a retrospective study. Eur. J. Neurol *19*, 1518–1524.

14. Aboussouan, L.S., Khan, S.U., Meeker, D.P., Stelmach, K., and Mitsumoto, H. (1997). Effect of noninvasive positive-pressure ventilation on survival in amyotrophic lateral sclerosis. Ann. Intern. Med. *127*, 450–453.

15. Rosen, D.R., Siddique, T., Patterson, D., Figlewicz, D.A., Sapp, P., Hentati, A., Donaldson, D., Goto, J., O'Regan, J.P., Deng, H.X., et al. (1993). Mutations in Cu/Zn superoxide dismutase gene are associated with familial amyotrophic lateral sclerosis. Nature *362*, 59–62.

16. Gurney, M.E., Pu, H., Chiu, A.Y., Dal Canto, M.C., Polchow, C.Y., Alexander, D.D., Caliendo, J., Hentati, A., Kwon, Y.W., Deng, H.X., et al. (1994). Motor neuron degeneration in mice that express a human Cu,Zn superoxide dismutase mutation. Science *264*, 1772–1775.

17. Nimchinsky, E.A., Young, W.G., Yeung, G., Shah, R.A., Gordon, J.W., Bloom, F.E., Morrison, J.H., and Hof, P.R. (2000). Differential vulnerability of oculomotor, facial, and hypoglossal nuclei in G86R superoxide dismutase transgenic mice. J. Comp. Neurol. *416*, 112–125.

18. Stoica, L., Keeler, A.M., Xiong, L., Kalfopoulos, M., Desrochers, K., Brown, R.H., Jr., Sena-Esteves, M., Flotte, T.R., and ElMallah, M.K. (2017). Restrictive lung disease in the Cu/Zn superoxide-dismutase 1 G93A amyotrophic lateral sclerosis mouse model. Am. J. Respir. Cell Mol. Biol. *56*, 405–408.

19. Tankersley, C.G., Haenggeli, C., and Rothstein, J.D. (2007). Respiratory impairment in a mouse model of amyotrophic lateral sclerosis. J. Appl. Physiol. (1985) *102*, 926–932.

20. Smittkamp, S.E., Brown, J.W., and Stanford, J.A. (2008). Time-course and characterization of orolingual motor deficits in B6SJL-Tg(SOD1-G93A)1Gur/J mice. Neuroscience *151*, 613–621.

21. Nichols, N.L., Gowing, G., Satriotomo, I., Nashold, L.J., Dale, E.A., Suzuki, M., Avalos, P., Mulcrone, P.L., McHugh, J., Svendsen, C.N., and Mitchell, G.S. (2013). Intermittent hypoxia and stem cell implants preserve breathing capacity in a rodent model of amyotrophic lateral sclerosis. Am. J. Respir. Crit. Care Med. *187*, 535–542.

22. Stoica, L., Todeasa, S.H., Cabrera, G.T., Salameh, J.S., ElMallah, M.K., Mueller, C., Brown, R.H., Jr., and Sena-Esteves, M. (2016). Adeno-associated virus-delivered artificial microRNA extends survival and delays paralysis in an amyotrophic lateral sclerosis mouse model. Ann. Neurol. *79*, 687–700.

23. Borel, F., Gernoux, G., Cardozo, B., Metterville, J.P., Toro Cabrera, G.C., Song, L., Su, Q., Gao, G.P., Elmallah, M.K., Brown, R.H., Jr., and Mueller, C. (2016). Therapeutic rAAVrh10 mediated *SOD1* silencing in adult *SOD1*^{G93A} mice and nonhuman primates. Hum. Gene Ther. *27*, 19–31.

24. Borel, F., Gernoux, G., Sun, H., Stock, R., Blackwood, M., Brown, R.H., Jr., and Mueller, C. (2018). Safe and effective superoxide dismutase 1 silencing using artificial microRNA in macaques. Sci. Transl. Med. *10*, eaau6414.

25. ElMallah, M.K., Falk, D.J., Lane, M.A., Conlon, T.J., Lee, K.Z., Shafi, N.I., Reier, P.J., Byrne, B.J., and Fuller, D.D. (2012). Retrograde gene delivery to hypoglossal motoneurons using adeno-associated virus serotype 9. Hum. Gene Ther. Methods *23*, 148–156.

26. Elmallah, M.K., Falk, D.J., Nayak, S., Federico, R.A., Sandhu, M.S., Poirier, A., Byrne, B.J., and Fuller, D.D. (2014). Sustained correction of motoneuron histopathology following intramuscular delivery of AAV in pompe mice. Mol. Ther. *22*, 702–712.

27. Falk, D.J., Mah, C.S., Soustek, M.S., Lee, K.Z., Elmallah, M.K., Cloutier, D.A., Fuller, D.D., and Byrne, B.J. (2013). Intrapleural administration of AAV9 improves neural and cardiorespiratory function in Pompe disease. Mol. Ther. *21*, 1661–1667.

28. Hatzipetros, T., Kidd, J.D., Moreno, A.J., Thompson, K., Gill, A., and Vieira, F.G. (2015). A quick phenotypic neurological scoring system for evaluating disease progression in the SOD1-G93A mouse model of ALS. J. Vis. Exp *104*, 53257.

29. Biferi, M.G., Cohen-Tannoudji, M., Cappelletto, A., Giroux, B., Roda, M., Astord, S., Marais, T., Bos, C., Voit, T., Ferry, A., et al. (2017). A new AAV10-U7-mediated gene therapy prolongs survival and restores function in an ALS mouse model. Mol. Ther *25*, 2038–2052.

30. Kaspar, B.K., Lladó, J., Sherkat, N., Rothstein, J.D., and Gage, F.H. (2003). Retrograde viral delivery of IGF-1 prolongs survival in a mouse ALS model. Science *301*, 839–842.

31. Dodge, J.C., Haidet, A.M., Yang, W., Passini, M.A., Hester, M., Clarke, J., Roskelley, E.M., Treleaven, C.M., Rizo, L., Martin, H., et al. (2008). Delivery of AAV-IGF-1 to the CNS extends survival in ALS mice through modification of aberrant glial cell activity. Mol. Ther *16*, 1056–1064.

32. Lin, H., Hu, H., Duan, W., Liu, Y., Tan, G., Li, Z., Liu, Y., Deng, B., Song, X., Wang, W., et al. (2018). Intramuscular delivery of scAAV9-hIGF1 prolongs survival in the hSOD1^{G93A} ALS mouse model via upregulation of D-amino acid oxidase. Mol. Neurobiol. *55*, 682–695.

33. Wang, W., Wen, D., Duan, W., Yin, J., Cui, C., Wang, Y., Li, Z., Liu, Y., and Li, C. (2018). Systemic administration of scAAV9-IGF1 extends survival in SOD1^{G93A} ALS mice via inhibiting p38 MAPK and the JNK-mediated apoptosis pathway. Brain Res. Bull. *139*, 203–210.

34. Zhang, H., Yang, B., Mu, X., Ahmed, S.S., Su, Q., He, R., Wang, H., Mueller, C., Sena-Esteves, M., Brown, R., et al. (2011). Several rAAV vectors efficiently cross the blood-brain barrier and transduce neurons and astrocytes in the neonatal mouse central nervous system. Mol. Ther *19*, 1440–1448.

35. Piguet, F., Sondhi, D., Piraud, M., Fouquet, F., Hackett, N.R., Ahouansou, O., Vanier, M.T., Bieche, I., Aubourg, P., Crystal, R.G., et al. (2012). Correction of brain oligodendrocytes by AAVrh.10 intracerebral gene therapy in metachromatic leukodystrophy mice. Hum. Gene Ther. *23*, 903–914.

36. Ralph, G.S., Radcliffe, P.A., Day, D.M., Carthy, J.M., Leroux, M.A., Lee, D.C., Wong, L.F., Bilsland, L.G., Greensmith, L., Kingsman, S.M., et al. (2005). Silencing mutant SOD1 using RNAi protects against neurodegeneration and extends survival in an ALS model. Nat. Med. *11*, 429–433.

37. Sengupta-Ghosh, A., Dominguez, S.L., Xie, L., Barck, K.H., Jiang, Z., Earr, T., Imperio, J., Phu, L., Budayeva, H.G., Kirkpatrick, D.S., et al. (2019). Muscle specific kinase (MuSK) activation preserves neuromuscular junctions in the diaphragm but is not sufficient to provide a functional benefit in the SOD1^{G93A} mouse model of ALS. Neurobiol. Dis. *124*, 340–352.

38. Remmers, J.E., deGroot, W.J., Sauerland, E.K., and Anch, A.M. (1978). Pathogenesis of upper airway occlusion during sleep. J. Appl. Physiol. *44*, 931–938.

39. Bailey, E.F., and Fregosi, R.F. (2004). Coordination of intrinsic and extrinsic tongue muscles during spontaneous breathing in the rat. J. Appl. Physiol. *96*, 440–449.

40. Gestreau, C., Dutschmann, M., Obled, S., and Bianchi, A.L. (2005). Activation of XII motoneurons and premotor neurons during various oropharyngeal behaviors. Respir. Physiol. Neurobiol. *147*, 159–176.

41. Fuller, D., Mateika, J.H., and Fregosi, R.F. (1998). Co-activation of tongue protrudor and retractor muscles during chemoreceptor stimulation in the rat. J. Physiol. *507*, 265–276.

42. Fuller, D.D., Williams, J.S., Janssen, P.L., and Fregosi, R.F. (1999). Effect of co-activation of tongue protrudor and retractor muscles on tongue movements and pharyngeal airflow mechanics in the rat. J. Physiol. *519*, 601–613.

43. Keeler, A.M., Zieger, M., Todeasa, S.H., McCall, A.L., Gifford, J.C., Birsak, S., Choudhury, S.R., Byrne, B.J., Sena-Esteves, M., and ElMallah, M.K. (2019). Systemic delivery of AAVB1-GAA clears glycogen and prolongs survival in a mouse model of Pompe disease. Hum. Gene Ther. *30*, 57–68.

44. Drorbaugh, J.E., and Fenn, W.O. (1955). A barometric method for measuring ventilation in newborn infants. Pediatrics *16*, 81–87.

45. Keeler, A.M., Liu, D., Zieger, M., Xiong, L., Salemi, J., Bellvé, K., Byrne, B.J., Fuller, D.D., ZhuGe, R., and ElMallah, M.K. (2017). Airway smooth muscle dysfunction in Pompe ($Gaa^{-/-}$) mice. Am. J. Physiol. Lung Cell. Mol. Physiol. *312*, L873–L881.

46. Robichaud, A., Fereydoonzad, L., and Schuessler, T.F. (2015). Delivered dose estimate to standardize airway hyperresponsiveness assessment in mice. Am. J. Physiol. Lung Cell. Mol. Physiol. *308*, L837–L846.

47. Valdez, G., Tapia, J.C., Kang, H., Clemenson, G.D., Jr., Gage, F.H., Lichtman, J.W., and Sanes, J.R. (2010). Attenuation of age-related changes in mouse neuromuscular synapses by caloric restriction and exercise. Proc. Natl. Acad. Sci. USA *107*, 14863–14868.

48. Taetzsch, T., Tenga, M.J., and Valdez, G. (2017). Muscle fibers secrete FGFBP1 to slow degeneration of neuromuscular synapses during aging and progression of ALS. J. Neurosci. *37*, 70–82.